Simulation of aperture-optimised refractive lenses for hard X-ray full field microscopy

Felix Marschall,[1,2] **Arndt Last,**[1,*] **Markus Simon,**[1,3] **Harald Vogt,**[1,4] **and Jürgen Mohr**[1]

[1]*Institute of Microstructure Technology (IMT), Karlsruhe Institute of Technology (KIT), Hermann-von-Helmholtz-Platz 1, 76344 Eggenstein-Leopoldshafen, Germany*
[2]*Current affiliation: Paul Scherrer Institut, 5232 Villigen PSI, Switzerland*
[3]*Current affiliation: Pi miCos GmbH, Freiburger Straße 30, 79427 Eschbach, Germany*
[4]*Current affiliation: MA micro automation GmbH, Opelstr. 1, 68789 St. Leon-Rot, Germany*
[*]*arndt.last@kit.edu*

Abstract: The aperture of refractive X-ray lenses is limited by absorption and geometry. We introduce a specific simulation method to develop an aperture-optimized lens design for hard X-ray full field microscopy. The aperture-optimized lens, referred to as Taille-lens, allows for high spatial resolution as well as homogeneous image quality. This is achieved by the individual adaptation of the apertures of hundreds of lens elements of an X-ray imaging lens to the respective microscopy setup. For full field microscopy, the simulations result in lenses with both a large entrance and exit aperture and lens elements with smaller apertures in the middle of the lens.

OCIS codes: (080.2740) Geometric optical design; (080.3620) Lens system design; (120.3620) Lens system design; (180.7460) X-ray microscopy; (220.2740) Geometric optical design; (340.7460) X-ray microscopy

References and links

1. T. Tomie, "X-ray lens," Japanese patent 6-045288 (February 18, 1994); U.S. patents 5,594,773 (January 14, 1997) and 5,684,852 (November 4, 1997).
2. A. Snigirev, V. Kohn, I. Snigireva and B. Lengeler, "A compound refractive lens for focusing high-energy x-rays," Nature **384**, 49–51 (1996).
3. B. Lengeler, C. G. Schroer, M. Kuhlmann, B. Benner, T. F. Gunzler, O. Kurapova, A. Somogyi, A. Snigirev and I. Snigireva, "Beryllium parabolic refractive x-ray lenses," AIP Conf Proc **705**, 748-751 (2004).
4. B. Lengeler, C. G. Schroer, B. Benner, A. Gerhardus, T. F. Gunzler, M. Kuhlmann, J. Meyer and C. Zimprich, "Parabolic refractive x-ray lenses," J. Synchrotron Rad. **9**, 119-124 (2002).
5. A. Stein, K. Evans-Lutterodt, N. Bozovic and A. Taylor, "Fabrication of silicon kinoform lenses for hard x-ray focusing by electron beam lithography and deep reactive ion etching," J. Vac. Sci. Technol. B **26** (1), 122-127 (2008).
6. B. Nhammer, C. David, H. Rothuizen, J. Hoszowska and A. Simionovici,"Deep reactive ion etching of silicon and diamond for the fabrication of planar refractive hard x-ray lenses," Microelectron Eng. **67–68**, 453–460 (2003).
7. Y. Ohishi, A. Q. R. Baron, M. Ishii, T. Ishikawa, and O. Shimomura, "Refractive x-ray lens for high pressure experiments at SPring-8," Nucl. Instr. Meth. Phys. Res. A **467–468**, 962–965 (2001).
8. F. Marschall, A. Last, M. Simon, M. Kluge, V. Nazmov, H.Vogt, M. Ogurreck, I. Greving and J. Mohr, "X-ray full field microscopy at 30 keV," J. Phys.: Conf. Ser. **499**, 012007, (2014).
9. E. Reznikova, T. Weitkamp, V. Nazmov, M. Simon, A. Last and V. Saile, "Transmission hard x-ray microscope with increased view field using planar refractive objectives and condensers made of SU-8 polymer," J. Phys.: Conf. Ser. **186**, 012070 (2009).

#259855 Received 23 Feb 2016; revised 20 Apr 2016; accepted 3 May 2016; published 10 May 2016

10. V. Nazmov, E. Reznikova, A. Last, J. Mohr, V. Saile, M. DiMichiel and J. Gttert, "Crossed planar x-ray lenses made from nickel for x-ray micro focusing and imaging applications", Nucl. Instr. Meth. Phys. Res. A, **582**, 120-122 (2007).
11. A. Snigirev, I. Snigireva, G. Vaughan, J. Wright, M. Rossat, A. Bytchkov and C. Curfs, "High energy x-ray transfocator based on Al parabolic refractive lenses for focusing and collimation," J. Phys.: Conf. Ser. **186**, 012073 (2009).
12. C. G. Schroer and B. Lengeler, "Focusing hard x-rays to nanometer dimensions by adiabatically focusing lenses," Phys. Rev. Lett. **94**, 054802 (2005).
13. C. G. Schroer, T. F. Gnzler, B. Benner, M. Kuhlmann, J. Tmmler, B. Lengeler, C. Rau, T. Weitkamp, A. Snigirev and I. Snigireva, "Hard x-ray full field microscopy and magnifying microtomography using compound refractive lenses," Nucl. Instr. Meth. Phys. Res. A **467–468**, 966-969 (2001).
14. Kohn, V. G., "An exact theory of imaging with a parabolic continuously refractive x-ray lens," J. Exp. Theor. Phys. **97**, 204-215 (2003).
15. V. Saile, *LIGA and Its Applications* (Wiley-VCH Verlag GmbH & Co. KGaA, 2008).
16. A. Thompson, I. Lindau, D. Attwood, Y. Liu, and H. Winick, "X-ray data booklet," Lawrence Berkeley National Lab, http://xdb. lbl. gov (2009).
17. R. Simon, V. Nazmov, E. Reznikova, J. Mohr, and V. Saile, "Hard x-ray imaging and microscopy with lithographic CRL developed at ANKA synchrotron radiation facility," IPAP Conf. Series **7**,115–116 (2005).

1. Introduction

Refractive x-ray lenses for x-ray imaging consist of a large number of single lens elements. They have been described first in [1,2]. Today, they are fabricated from beryllium [3], aluminum [4], silicon [5], diamond [6], photoresist [7–9] and other materials. The most common type of x-ray lens, used in many applications [8–11], consists of many identical, biconcave, parabolic lens elements.

For special applications the geometry of the lens elements can also be varied, like in case of adiabatic lenses [12]. These lenses are optimized for illuminating a small point by varying apertures and radii along the optical axis. The adaptation of the apertures to the ray path results in a large numerical exit aperture and in a small focal point, which is beneficial in scanning microscopy [10].

In full field microscopy, lenses have to fulfill the request for a high numerical aperture for all points in the field of view. This is necessary to achieve high and homogeneous resolution and brightness in the entire image. The aperture of x-ray lenses is small compared to their length and often even smaller than the field of view. Thus, calculating the numerical aperture for only one point on the optical axis is not sufficient. Accordingly, we simulated the entrance acceptance angle and the ray path inside a refractive lens for every point of the field of view.

Analysing the ray path inside a lens leads us to adapting the apertures of the lens elements, in such a way that the entrance acceptance angle increases. This leads to an increase in intensity. Additionally the intensity distribution becomes significantly more homogeneous in the field of view. The resulting lens has a bigger entrance and exit aperture whereas lens elements in the middle of the lens have smaller apertures. The overall shape of the resulting lens geometry was the reason for choosing the name Taille-lenses (German for waist). Using this lenses one can achieve better image quality in hard x-ray full field microscopy compared to lenses with constant aperture.

2. Lenses for full field microscopy

As it is known from visible light full field microscopy, it is essential to illuminate and to image every point of the field of view with equal intensity and equal angular range. Illumination and imaging angles are chosen dependent on the sample and the contrast mechanism. In contrast to visible light optics, the refractive power of x-ray lenses is weak for all lens materials. Many strongly curved surfaces are required to achieve the desired focal length [1]. Hence, a refractive x-ray is lens long compared to its aperture. Additionally, in -ray full field microscopy the

#259855 Received 23 Feb 2016; revised 20 Apr 2016; accepted 3 May 2016; published 10 May 2016

aperture of the objective lens is often even smaller than the field of view.

The aperture of x-ray imaging lenses is limited by both, absorption and geometry. The absorption limited aperture, which is also called effective aperture D_{eff}, is described [13] as

$$D_{eff} = 4\sqrt{\frac{f\delta}{\mu}}, \tag{1}$$

with the focal length f, the decrement of the refractive index δ, and the attenuation coefficient μ. The geometry limited aperture D_g can be written as

$$D_g = 2\sqrt{\frac{(L - Nd - (N-1)a)r}{N}}, \tag{2}$$

and is a result of the length L of the lens

$$L = 2N\frac{1}{2r}\left(\frac{D_g}{2}\right)^2 + (N-1)a + Nd, \tag{3}$$

with the radius in the apex of the parabola r, the distance between the two parabolic surfaces of one lens element d, the distance between two lens elements a, and the number of lens elements N (see Fig. 1(a). The number of lens elements N can be calculated [14] from the focal length f

$$f = \frac{r}{2\delta N} + \frac{L}{6}. \tag{4}$$

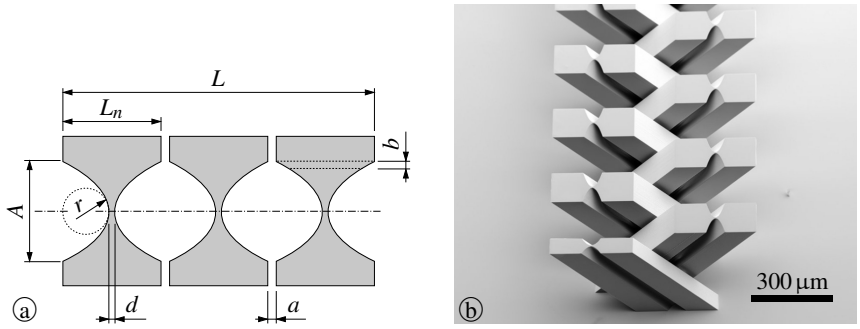

Fig. 1. Schematic (a) and SEM image (b) of an x-ray imaging lens: L – length of one lens element, A – aperture, r – radius in the apex of the parabola, d – smallest thickness of one lens element, a – distance between two lens elements, b = width of the boundary area (1 % of local aperture)

As an example, we simulated parabolic imaging lenses, using parameters derived from a lens manufactured by deep x-ray lithography from mr-L negative resist [15]. Such lenses consist of many extruded lens elements in an alternating crossed assembly [9] (s. Fig. 1(b)). As a result of the current fabrication process at the Institute of Microstructure Technology, the length of the lenses is limited to 60mm, but can also be limited by the available space in the microscope setup. We choose a focal length f of 100mm, which turned out to be suitable for the calcu-lated example of an x-ray microscope for imaging a field of view of 100µm× 100µm with a resolution better than 100nm.

The calculated results of the absorption and geometry limited apertures are shown in Fig. 2. For lower photon energies absorption is the limiting factor. For higher photon energies the

#259855 Received 23 Feb 2016; revised 20 Apr 2016; accepted 3 May 2016; published 10 May 2016

aperture is limited by geometry due to the restriction of the lens length L. Above 30.5 keV the absorption limited aperture decreases again, due to the absorption edge of antimony, which is used as photo initiator in the mr-L negative resist [16]. We choose 30 keV photon energy for our calculations, because at this energy the absorption limited aperture and consequently the potential for improvements due to geometry variations is largest. In addition, lenses fabricated out of mr-L negative resist show a good performance in this energy range [17].

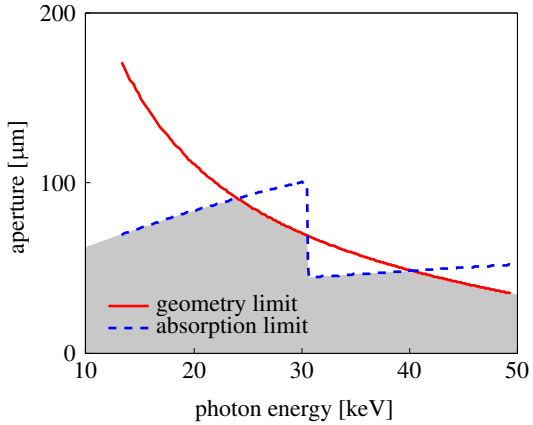

Fig. 2. Comparison of absorption and geometry limited aperture of a refractive x-ray lens for different photon energies. For calculation we assume a lens from mr-L negative resist with alternating crossed lens elements, 60 mm lens length, 100 mm focal length and 6 µm radius of the parabola in the apex.

3. Acceptance angle of x-ray imaging lenses for full field microscopy

The numerical aperture NA is directly linked to the acceptance angle α and can be calculated from the aperture and the focal length. A big numerical aperture NA is essential for a high resolution. Generally, the resolution is described by the smallest distance d_{min} of two objects, which are just resolvable

$$d_{\mathrm{min}} = \frac{\lambda}{2NA} = \frac{\lambda}{2\sin(\alpha/2)}. \tag{5}$$

As a result of the huge length of x-ray lenses in comparison to their aperture, it is not sufficient to characterise an x-ray imaging lens for full field microscopy by only one value for the numerical aperture. The deviation of the acceptance angle for points close to the edge of the field of is not negligible. Thus it is necessary to calculate the acceptance angle for all points in the field of view.

We simulated a lens fabricated from mr-L negative resist for 30 keV consisting of 249 alternating crossed lens elements in total, which means 124 lens elements for horizontal and 125 lens elements for vertical refraction. All lens elements have a 6 µm radius in the apex of the parabola and an aperture of 70 µm. As the vertical direction has one lens element more, the first and the last one have a doubled radius in the apex and consequently half refractive power. So, in total the lens elements for horizontal and vertical refraction have the same refractive power. Due to the unequal number, it is possible to arrange the lens elements for both directions symmetrical around the same centre. Thus, the principal planes for both directions match, which avoids astigmatism and unequal magnification in horizontal and vertical direction, respectively.

#259855 Received 23 Feb 2016; revised 20 Apr 2016; accepted 3 May 2016; published 10 May 2016

The acceptance angle α of this lens for each point in the field of view as a function of the distance to the optical axis is shown in Fig. 3. Additionally, we added the angles α_t of the top most and α_b the lowest ray passing the lens for each point. The result of the simulation is nearly equal in horizontal and vertical direction. The acceptance angle decreases significantly from the centre to the edges of the field of view. Consequently, the achievable resolution is 62 nm in the centre and 89 nm at the edges of the field of view. The angles of the top most and the lowest ray for all points are point symmetric as a result of the symmetry of the lens.

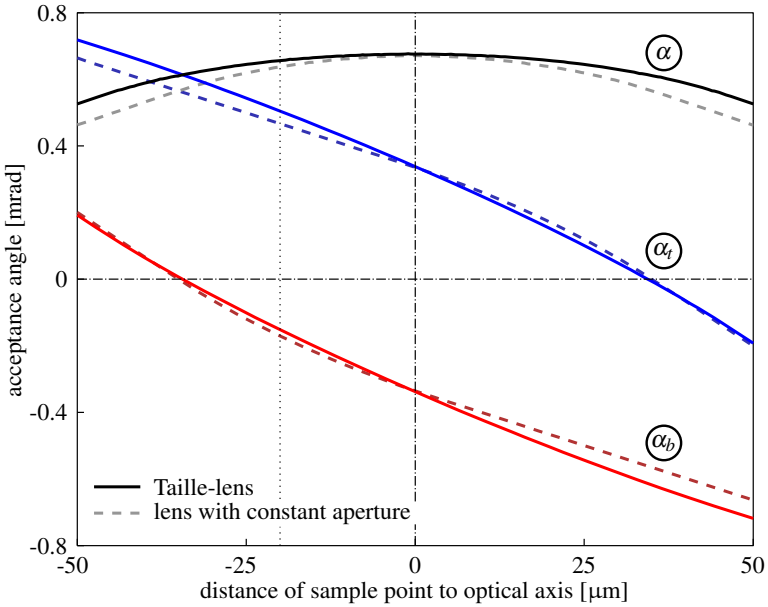

Fig. 3. Comparison of the acceptance angle (α), as well as angle of the top most (α_t) and lowest (α_b) ray of an x-ray lens with constant aperture and a Taille-lens dependent on the distance to the optical axis.

Besides the size also the direction of the accepted angular range is changing from the centre to the edges of the field of view. This can be seen in the curvatures of the top most and lowest ray and is a result of the small entrance aperture in comparison to the field of view. However, the resolution is affected only marginally by the direction of the acceptance angle, if the illumination is adapted to the acceptance angle of the imaging lens. The main factor influencing the resolution is the size of the accepted angular range, which we optimized in our simulations.

The aperture of the lens is square shaped, due to the crossed assembly of the lens elements. Thus, the horizontal acceptance angle is independent from the vertical position of the individual sample point and the vertical acceptance angle is independent from the horizontal position. However, the results are very similar for rotational symmetric lenses. As the absorption limited aperture of this lens is 100 µm, which is clearly bigger than the real aperture of 70 µm, we neglected the Gaussian transmission profile of the lens for the calculation of the theoretical resolution. The transmission of a ray along the optical axes is 92 %. The intensity of the ray with the lowest transmission in the simulation for Fig. 3 was 37 %.

4. Photon density distribution in x-ray lenses

For optimizing the acceptance angle of a lens, we verified the contribution of each part of the lens to the image formation by calculating the number of transmitted photons for each volume

#259855 Received 23 Feb 2016; revised 20 Apr 2016; accepted 3 May 2016; published 10 May 2016

element of the lens. The simulation was done with MATLAB using geometric ray optics. The resulting photon density distribution for our example of a lens with a constant aperture of 70 µm, a focal length of 100mm at 30keV for imaging a field of view of 100µm × 100µm with a magnification of 15, is plotted in Fig. 4(a).

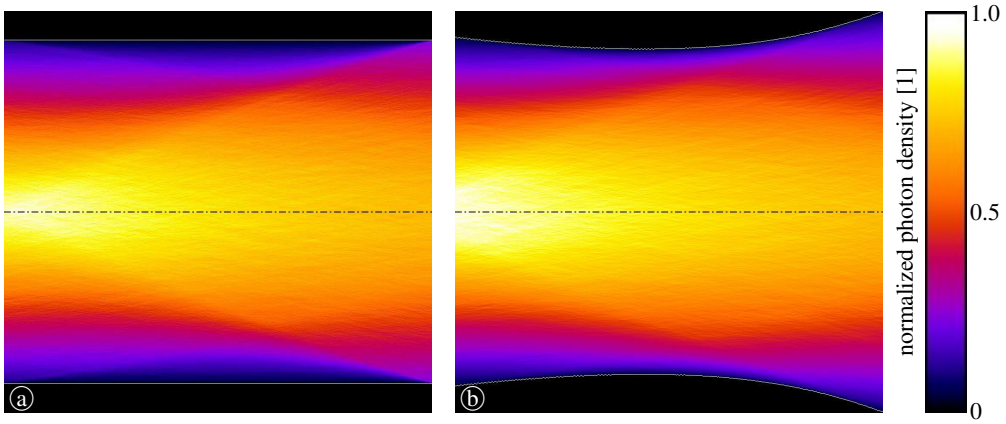

Fig. 4. Photon density distribution: a) of a lens with a constant aperture of 70 µm and b) of a Taille-lens with variable aperture (entrance aperture 71.5 µm, smallest aperture 66 µm, exit aperture 82 µm). Both lenses have a focal length of 100 mm at 30 keV. The source with a size of 100 µm × 100 µm is on the left with a distance of 106, 7 mm to the entrance principle plane. This is the sample distance for a magnification of 15. The axes scaling is unequal in this drawing. The horizontal edge length of the images is 60 mm, which is the length of the lens. The vertical edge length is 82 µm like the exit aperture of the Taille-lens.

Our simulations show, that the photon density is non-uniform. Naturally, it is much higher in the parts of the lens close to the optical axis than close to the edges of the apertures. This is a result of the lower absorption in the thinner parts of the lens elements close to the optical axis. However, the gradient of the photon density parallel to the optical axis is more interesting. Especially at the edges of the apertures the non-uniform photon density is conspicuous. The edges of the entrance and exit aperture have a higher photon density than the edges of the lens elements in the middle of the lens. We conclude that the edges of these lens elements are more relevant for imaging, than the edges of the lens elements in the middle of the lens.

Accordingly we iteratively optimized a lens in such a way, that the photon density at the edges of the local apertures became more uniform along the lens. This is achieved by varying the apertures of the individual lens elements. The apertures of lens elements with lower photon density at the edges are reduced. Consequently these lens elements become shorter. Under the constraint of a fixed total length of the lens, the resulting available space is used to enlarge the apertures of lens elements with a higher photon density at the edges. As this is only a slight variation of the apertures, the radius in the apex is kept constant.

The result of our calculations is a lens with an entrance aperture of 71.5 µm, smallest aperture of 66µm in the middle of the lens and an exit aperture of 82µm. The photon density distribution for such a Taille-lens design shown in Fig. 4(b) is more uniform compared to a lens with a constant aperture. Please note that the calculations of the photon density distribution as well as the optimized shape of the lens are only valid for the parameters we choose for our calculations.

An important parameter for calculating the required change of the local lens apertures is the width of the boundary area b of the lens elements (see Fig. 1). The best result is achieved with a boundary area as small as possible. However, as the computing time approaches infinity, when

#259855 Received 23 Feb 2016; revised 20 Apr 2016; accepted 3 May 2016; published 10 May 2016

the size of the boundary area approaches zero, the resulting shape is always a compromise between computing time and optimal properties of the lens. For the current Taille-lenses, we choose 1 % of the size of the local aperture A as width b for the boundary area. A further decrease shows only marginal improvements, but strongly increases computing time.

For a well-known optical setup, there are quicker ways of calculation, for example due to geometric dependencies. Anyway, with the concept using the photon density distribution it is possible to optimize a system without a priori knowledge. Additionally the concept is valid for all setups. For example, for a point source and a high demagnification the result is identical with an adiabatic lens.

5. Theoretical characterization of the aperture optimised Taille-lens

Taille-lenses have an increased acceptance angle for all points in the field of view compared to a lens with constant aperture, as it is shown in Fig. 3. For sample points near the optical axis the gain is small, but becomes significant for points in the outer area of the field of view. We calculated an average increase of the entrance acceptance angle of 5 % and an increase of 12 % at the edges of the field of view. Thus, the resolution is increased from 62 nm to 60 nm in the centre of the field of view and from 89 nm to 78 nm at the edges.

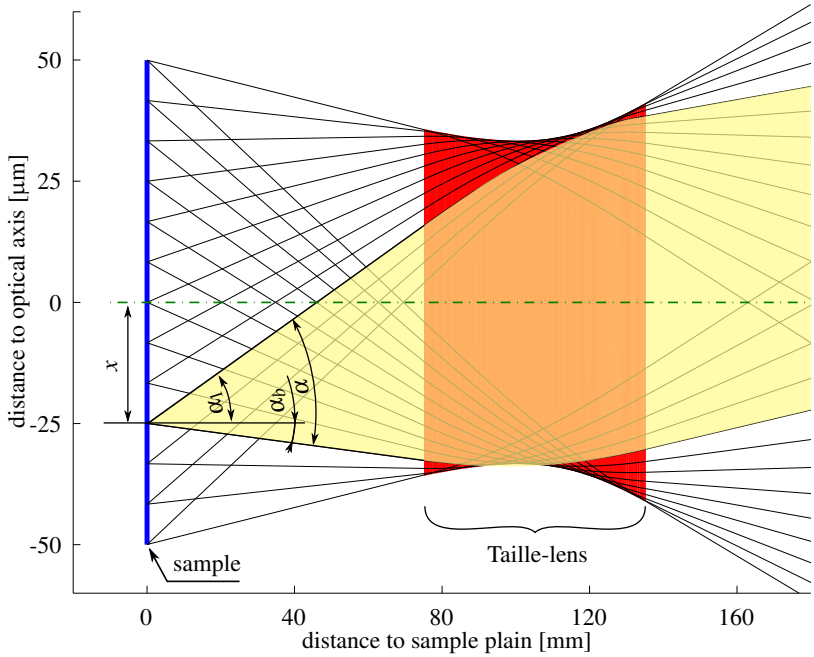

Fig. 5. Ray path through a Taille-lens for different points in the field of view. For each point the top most and the lowest ray is drawn. The angular range between the two rays defines the entrance acceptance angle α of the lens for the current point. The Taille-lens is drawn in red. The axes scaling is unequal, so that the single lens elements are not detectable and only the outer shape of the lens is visible. The yellow area represents all transmitted rays starting at the point x.

The acceptance angle for points in the outer areas of the field of view is not as good as for points in the centre. However our calculations demonstrate a more homogeneous acceptance angle over the entire field of view due to the Taille-lens design. Consequently the resulting

#259855 Received 23 Feb 2016; revised 20 Apr 2016; accepted 3 May 2016; published 10 May 2016

image shows a more homogeneous resolution and brightness, which was the main goal of the optimization process.

Until now, our view was only on the acceptance angle, but now we will focus on the direction of the rays, which are accepted by the lens dependent on the point in the field of view. As the field of view is larger than the entrance aperture, the direction of the accepted rays cannot be equal for all points in the field of view. For visualisation, the top most and the lowest ray for several points in the field of view is drawn in Fig. 5. The envelope over all of these rays describes the shape of the lens as a result of the varying apertures along the optical axis.

For each point in the field of view drawn in Fig. 5 the angle of the top most α_t and lowest ray α_b is displayed in Fig. 3. The difference of these two angles is the entrance acceptance angle of the lens for the corresponding point in the field of view. The slope of the curvature of the top most and lowest rays shows the change of the direction of the accepted rays. This change is significant, even if the acceptance angle α stays nearly constant.

Besides increasing the entrance acceptance angle, the Taille-lens design also improves the spectral transmission of the lens. Fig 6 shows the simulated image of a completely homogeneous illuminated sample, taken with a lens with constant aperture and a Taille-lens, respectively. The size of the simulated sample was 100µm× 100µm. Beside a significantly increased homogeneity of the image brightness, the overall number of transmitted photons is increased by 3% for the Taille-lens compared to a lens with constant aperture.

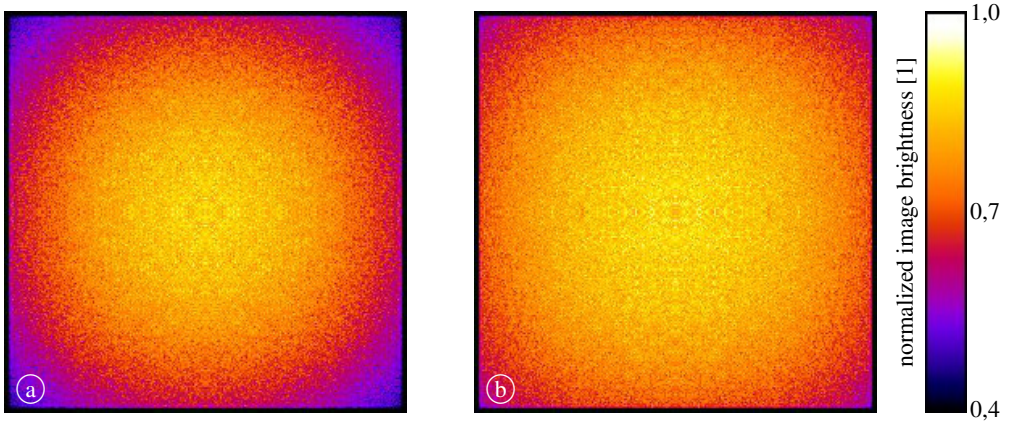

Fig. 6. Simulated brightness of the image of a completely homogeneous illuminated sample at 30 keV with (a) a lens with constant aperture and (b) a Taille-lens with varying aperture. Both lenses have a focal length of 100 mm, the field of view has a size of 100 µm × 100 µm and the magnification is 15.

The numerical aperture is determined by the aperture of the lens, the focal length and consequently the sample distance is also very important. Fig. 7 shows the simulated acceptance angle for Taille-lenses with focal lengths from 80 mm to 120 mm. All simulated lenses had a length of 60 mm. They were designed for a field of view of 100 µm × 100 µm, and a magnification of 15 at 30 keV. The acceptance angle for points in the centre of the field of view is increasing with decreasing focal length. This dependency was also the reason for developing adiabatic lenses, which are optimised for a small focal spot [12], due to a very short focal length and consequently a high acceptance angle for points on the optical axis.

Lenses with very short focal distance feature a small geometrical aperture. Using such a lens for full field microscopy results in a small field of view, because the acceptance angle for points distant to the optical axis decreases significantly with decreasing focal length. Thus, for full

#259855 Received 23 Feb 2016; revised 20 Apr 2016; accepted 3 May 2016; published 10 May 2016

field microscopy the focal length of the objective lens has to be chosen dependent on the size of the field of view. Evaluating the simulation result shown in Fig. 7, a focal length of 100 mm turned out to be a good compromise for imaging a field of view of 100 µm × 100 µm. This lens shows a high acceptance angle in the centre of the field of view, which is only slightly decreasing to the edges of the field of view. Anyway, this choice is always a compromise between maximum resolution, size of the field of view and homogeneity of the image.

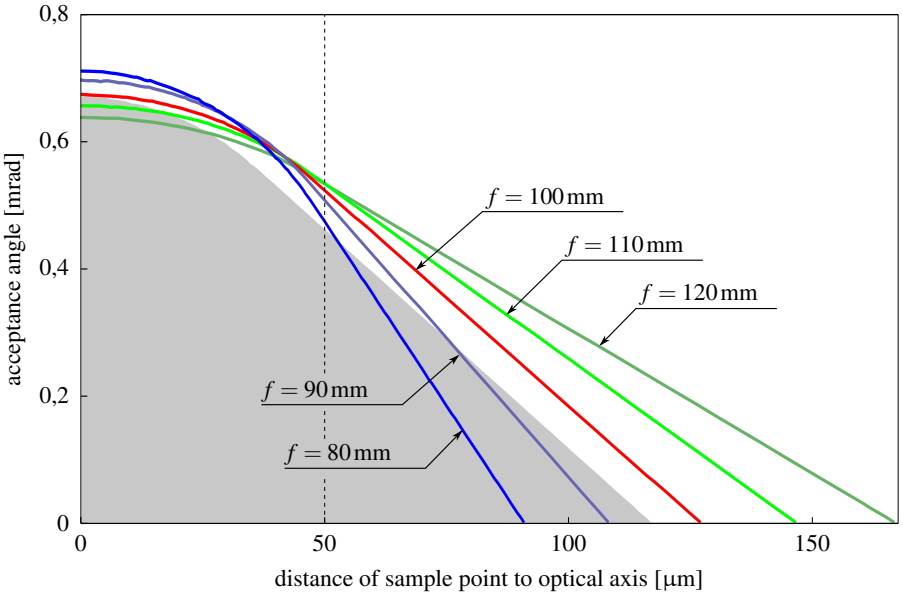

Fig. 7. Entrance acceptance angles of Taille-lenses with different focal lengths dependent on the distance of the sample point to the optical axis for a field of view of 100 µm × 100 µm

6. Conclusion

Taille-lenses are designed and optimized for imaging a large field of view in hard x-ray full field microscopy. They allow for a larger entrance acceptance angle for all points in the entire field of view, due to their shape with bigger entrance and exit apertures and smaller apertures in the middle of the lens. Especially for points close to the edge of the field of view, the improvement is significant.

As example, we calculated a microscope using lenses fabricated from SU-8 negative photo resist. But in principle the concept can also be applied to silicon lenses or approximated with beryllium lenses. For our example the resolution of an X-ray microscope is improved on average by 5 % and even by 12 % in the border areas of the field of view by using a Taille-lens, as a result of the increased entrance acceptance angle . Thus the resolution and the brightness of the image become more homogeneous over the entire field of view. Additionally the overall number of transmitted photons is increased by 3 %.

The development of Taille-lenses will improve the setup of future x-ray full field microscopes for photon energies above 15 keV. Especially for short assemblies, the resolution, the brightness and the homogeneity of the image gains significantly.

#259855 Received 23 Feb 2016; revised 20 Apr 2016; accepted 3 May 2016; published 10 May 2016

Acknowledgments

The authors thank the Karlsruhe Nano Micro Facility (KNMF), a Helmholtz Research Infrastructure for the possibility to fabricate the lenses with x-ray lithography. The work was performed within the Helmholtz Virtual Institute of New x-ray Analytic Methods in Material Science (VI-NXMM). We acknowledge support by Deutsche Forschungsgemeinschaft and Open Access Publishing Fund of Karlsruhe Institute of Technology.

#259855 Received 23 Feb 2016; revised 20 Apr 2016; accepted 3 May 2016; published 10 May 2016